

# Seismic performance assessment of reinforced concrete bridge piers supported by laminated rubber bearings

T. H. Kim and Y. J. Kim

*Civil Engineering Research Team, Daewoo Institute of Construction Technology,  
60 Songjuk-dong, Jangan-gu, Suwon, Gyeonggi-do, 440-210, Korea*

H. M. Shin<sup>†</sup>

*Department of Civil and Environmental Engineering, Sungkyunkwan University,  
300 Cheoncheon-dong, Jangan-gu, Suwon, Gyeonggi-do, 440-746, Korea*

*(Received December 18, 2006, Accepted March 31, 2008)*

**Abstract.** This paper presents a nonlinear finite element procedure accounting for the effects of geometric as well as material nonlinearities for reinforced concrete bridge piers supported by laminated rubber bearings. Reinforced concrete bridge piers supported by laminated rubber bearings and carrying a cyclic load were analyzed by using a special purpose, nonlinear finite element program, RCAHEST. For reinforced concrete, the proposed robust nonlinear material model captures the salient response characteristics of the bridge piers under cyclic loading conditions and addresses with the influence of geometric nonlinearity on post-peak response of the bridge piers by transformations between local and global systems. Seismic isolator element to predict the behaviors of laminated rubber bearings is also developed. The seismic performance of reinforced concrete bridge piers supported by laminated rubber bearings is assessed analytically. The results show good correlation between the experimental findings and numerical predictions, and demonstrate the reliability and robustness of the proposed analytical model. Additionally, the studies and discussions presented in this investigation provide an insight into the key behavioral aspects of reinforced concrete bridge piers supported by laminated rubber bearings.

**Keywords:** reinforced concrete bridge piers; laminated rubber bearings; nonlinear material model; geometric nonlinearity; seismic isolator element; seismic performance.

---

## 1. Introduction

The base-isolation system using laminated rubber bearings is considered an efficient technology for mitigation of seismic damage of structures and equipments, and has proven to be reliable and cost-effective (Chen *et al.* 2006).

The most important feature of seismic isolation is that its increased flexibility increases the natural period of the structure. Because the period is increased beyond that of the earthquake, resonance

---

<sup>†</sup> Professor, Corresponding author, E-mail: [hmsin@skku.ac.kr](mailto:hmsin@skku.ac.kr)

and near-resonance are avoided and the seismic acceleration response is reduced (Skinner *et al.* 1993). However, the increased period and consequent increased flexibility is accompanied by an increase in displacement demand that must be accommodated within the flexible mount (AASHTO 1999).

The isolation system consists of a sliding bearing, which generates friction damping, and a rubber bearing, which generates the restoring force. The sliding bearing is composed of a Teflon plate and a stainless steel plate on each sliding surface. Rubber bearings have been frequently used in recent years. They are able to support large loads while sustaining large movements and they require little or no maintenance.

Base-isolation bearings have many good properties that are beneficial for seismic protection of bridges. When these seismic isolation systems are installed, sophisticated inelastic analysis method is required. But since the conventional inelastic analysis method takes into account only the bridge piers, it is hard to design seismic isolators which can cope with the interaction between the seismic isolators and bridge piers (Roeder and Stanton 1991, Juhn *et al.* 1992).

A seismic isolator that, due to its sliding property, cuts off the inertia force acting on the bridge pier, is being developed. The sliding bearings are velocity and vertical-load dependent; therefore, under the effect of vertical ground motions, the friction coefficient is expected to change greatly, affecting the horizontal earthquake response (Naeim and Kelly 1999).

The purpose of this study is to understand the relationship between the laminated rubber bearings and bridge piers with respect to their energy dissipation etc. and to propose an analysis procedure for isolated bridges. In a single unit, laminated rubber bearings provide the combined features of vertical load support, horizontal flexibility, and energy absorbing capacity required for the base isolation of structures from earthquake attacks.

This paper presents the theory and formulations for multi-directional orthotropic material models for the nonlinear analysis of reinforced concrete bridge piers supported by laminated rubber bearings. In addition to the material nonlinear properties, the geometric nonlinearity based on total Lagrangian formulation is taken into account in the nonlinear finite element analysis. The analysis uses of Green-Lagrange strain tensors and the second Piola-Kirchhoff stress tensors.

An evaluation method for the seismic performance of reinforced concrete bridge piers supported by laminated rubber bearings is proposed. The proposed method, uses a nonlinear finite element analysis program (RCAHEST, Reinforced Concrete Analysis in Higher Evaluation System Technology), developed by the authors (Kim and Shin 2001, Kim *et al.* 2002, 2003, 2005, 2006). A seismic isolator element is newly incorporated into the structural element library for RCAHEST so that it can be used to predict the inelastic behavior of reinforced concrete bridge piers supported laminated rubber bearings.

## 2. Nonlinear material model for reinforced concrete

The nonlinear material model for the reinforced concrete is composed of the models for concrete and a model for the reinforcing bars. Models for concrete may be divided into models for uncracked concrete, which is isotropic, and for cracked concrete. For cracked concrete, three models describe the behavior of concrete in the direction normal to the crack plane, in the direction of the crack plane, and in shear direction at crack plane, respectively. The basic and widely-known model adopted for crack representation is based on the non-orthogonal fixed-crack method of the smeared crack concept.

The approach using this model is practical for cyclic loads whose history needs to be recorded.

This section simply summarizes the model used in this study; details of the model used are given by the authors (Kim *et al.* 2002, 2003, 2005, 2006).

### 2.1 Model for uncracked concrete

The elasto-plastic and fracture model for the biaxial state of stress proposed by Maekawa and Okamura (1983) is used as the constitutive equation for uncracked concrete.

For uncracked concrete, the nonlinearity, anisotropy, and strain softening effects are expressed independent of the loading history. The equivalent stress-strain relation is given by

$$S = E_o K_o (\varepsilon_t^{eq} - \varepsilon_p^{eq}) \tag{1}$$

where  $S$  = equivalent stress;  $E_o$  = initial stiffness of concrete;  $K_o$  = fracture parameter for uncracked concrete;  $\varepsilon_t^{eq}$  = equivalent total strain; and  $\varepsilon_p^{eq}$  = equivalent plastic strain.

### 2.2 Model for cracked concrete

After concrete cracks, its behavior becomes anisotropic in the crack direction. In finite element computation, cracking marks the switch from the uncracked concrete routine to the cracked one, and stresses along the crack axis are calculated. The stress-strain relations are modeled by decomposing the stress and strain in directions parallel to, along, and normal to cracks, respectively. Thus, the constitutive law adopted for cracked concrete consists of tension stiffening, compression and shear transfer models (see Fig. 1).

A refined tension stiffening model is obtained by transforming the tensile stresses of concrete into a component normal to the crack. This model would give improved accuracy, especially when the

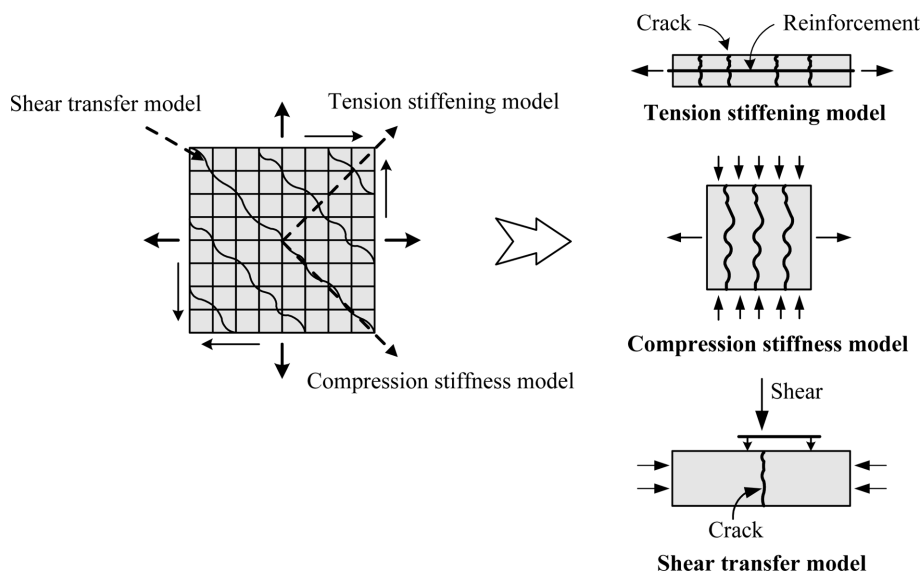


Fig. 1 Construction of cracked concrete model

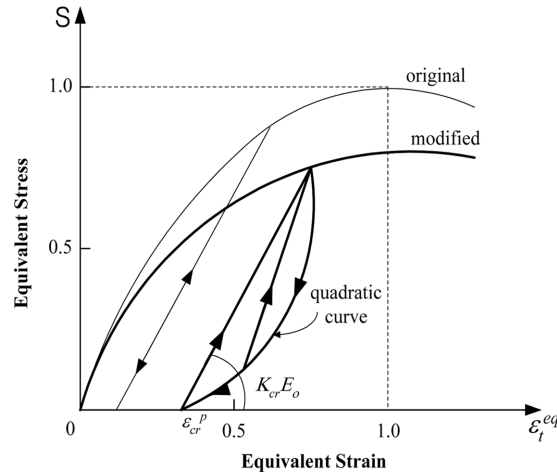


Fig. 2 Equivalent stress-equivalent strain relationship for concrete during unloading and reloading

reinforcing ratios in the orthogonal directions are significantly different and when the reinforcing bars are distributed only in one direction. The model proposed by Shima *et al.* (1987) is basically used as the tension stiffening model for unloading and reloading.

A modified elasto-plastic fracture model (Okamura *et al.* 1987) is used to describe the compressive behavior of the concrete struts in between cracks in the direction of the crack plane. The model describes the degradation in compressive stiffness by modifying the fracture parameter in terms of the strain perpendicular to the crack plane. The cyclic load damages the inner concrete, and energy is dissipated during unloading and reloading. This behavior is considered in the model. To consider this behavior, the model experimentally fits the stress-strain curve at unloading to the quadratic curve, as shown in Fig. 2.

The shear transfer model based on the contact surface density function (Li *et al.* 1989) is used to consider the effect on shear stress transfer due to the aggregate interlock at the crack surface. The contact surface is assumed to respond elasto-plastically, and the model is applicable to any arbitrary loading history. For the shear transfer model for unloading and reloading, the model modified by the authors (Kim *et al.* 2003) is used.

### 2.3 Model for the reinforcing bar in concrete

The modeling of the reinforcing bar in concrete must be based on the properties of the bare bar and the effect of the bonding between bar and concrete.

The stress acting on the reinforcing bar embedded in concrete is not uniform and the value is maximum at locations where the bar is exposed to a crack plane. The constitutive equations for the bare bar may be used if the stress strain relation is in the elastic range. The post-yield constitutive law for the reinforcing bar in concrete considers the bond characteristics, and the model is a bilinear model given by

$$\sigma_s^{av} = \sigma_{sh}^o + E_{sh}(\varepsilon_s^{av} - \varepsilon_{sh}^{av}) \quad (2)$$

where  $\sigma_s^{av}$  = average steel stress;  $\sigma_{sh}^o$  = offset stress point for the initiation of strain hardening of

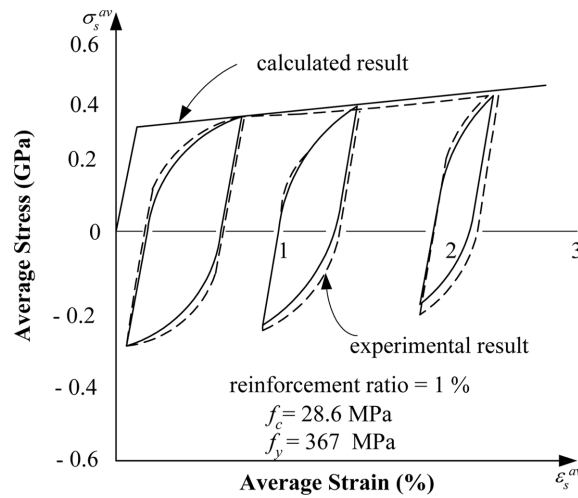


Fig. 3 Reinforcement model for reversed cyclic loading

the bar;  $\epsilon_s^{av}$  = average steel strain;  $\epsilon_{sh}^{av}$  = average steel strain for the offset point for the initiation of strain hardening; and  $E_{sh}$  = strain hardening rates of the bar embedded in concrete.

Kato's model (1979) for the bare bar under reversed cyclic loading and the assumption of a stress distribution denoted by a cosine curve were used to derive the mechanical behavior of reinforcing bars in concrete under reversed cyclic loading (see Fig. 3).

For reinforcing bars under extreme compression, the lateral bar buckling tends to occur, which greatly affects the post peak behavior and member ductility. To account for buckling of reinforcing bars, the average stress-strain behavior after concrete crushing is assumed to be linearly descending until the 20% average steel stress is reached (Kim *et al.* 2005).

#### 2.4 Models and assumptions for the interface

The local discontinuous deformation, which is a part of the anchorage slip, shear slip at the joint plane, and penetration at the joint plane, occurs according to the stiffness changing rapidly in the column and foundation etc. (see Fig. 4). Therefore, in order to predict the response of the structures

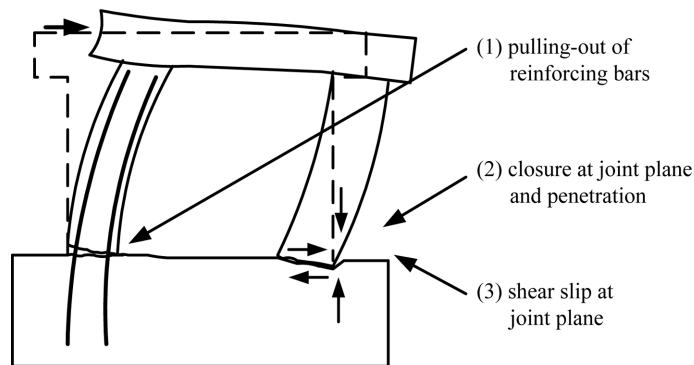


Fig. 4 Three types of localized discontinuous deformation at boundary plane

at the boundary plane with accuracy, the interface element is required.

The interface model for the boundary plane connecting two reinforced concrete elements with different sections is based on the discrete crack concept, which uses the relationships between the stress and the localized deformations. The model is one-dimensional and has no thickness (Kim *et al.* 2003).

### 2.5 Confinement in concrete by reinforcements

The transverse reinforcements confine the compressed concrete in the core region and inhibit the buckling of the longitudinal reinforcing bars. In addition, the reinforcements also improve the ductility capacity of the unconfined concrete.

This study adopted a model proposed by Mander *et al.* (1988). The models consider the yield strength, the distribution type, and the amount of the longitudinal and transverse reinforcing bars to compute the effective lateral confining stress and the ultimate compressive strength and strain of the confined concrete.

### 2.6 Model for fatigue damage

Fatigue damage of reinforced concrete bridge piers subjected to seismic load seems inevitable. Fatigue damage influencing the inelastic behavior of reinforced concrete bridge piers may be characterized as concrete strength deterioration and low cycle fatigue of reinforcing bars (Kim *et al.* 2005).

The formula of Kakuta *et al.* (1982) derived from plain concrete specimens tests is adopted for the fatigue model of concrete. The formula is modified so that it can be applied to reinforced concrete (Kim *et al.* 2005).

Reinforcing bars dominate the behavior of reinforced concrete members under seismic load. The plastic strain of reinforcing bars is an important variable of low cycle fatigue. This study applied the Coffin-Manson equation (Mander *et al.* 1994), which is modified so that it can be applied to reinforced concrete (Kim *et al.* 2005).

## 3. Finite element formulation with large displacement

Reinforced concrete bridge piers may undergo large displacement under earthquake loading. Thus, the geometry of structure may substantially change with the increase in loading (Yalcin and Saatcioglu 2000). Hence, the correct prediction of load-displacement behavior and structural stability, coupled material and geometrical nonlinearity must be considered (see Fig. 5).

Geometrical nonlinearity is considered by adopting the total Lagrangian formulation in which current (second Piola Kirchoff) stress and (Green-Lagrange) strain fields are defined in terms of the initial geometry while the displacement field is updated with respect to the current geometry (Bathe 1996).

Since the formulation refers to the original shape of the structure, it has the advantage of saving computational time for calculating the strain-displacement matrix. The linear part needs to be calculated only once but the nonlinear part needs to be updated using the current displacements.

$$\{\varepsilon\} = \{\varepsilon_l\} + \{\varepsilon_n\} \quad (3)$$

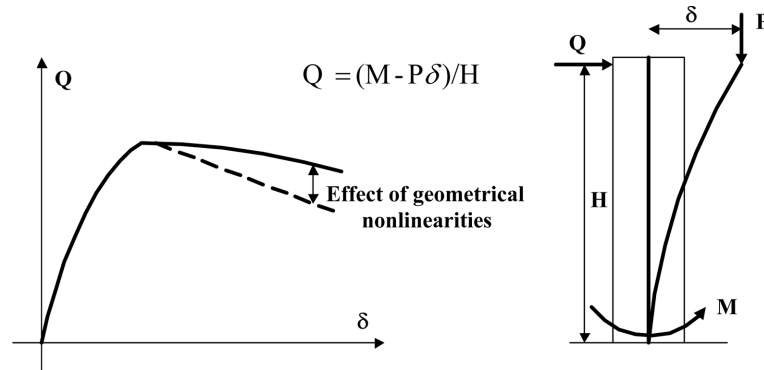


Fig. 5 Effect of geometrical nonlinearities in post-peak response

where  $\{\varepsilon\}$  = strain;  $\{\varepsilon_l\}$  = linear part of the strain obtained by linear differentiation of displacement; and  $\{\varepsilon_n\}$  = nonlinear part of the strain due to second-order terms.

The strain  $\{\varepsilon\}$  gives

$$\{\varepsilon\} = [B]\{d\} \tag{4}$$

where  $[B]$  = strain/displacement matrix; and  $\{d\}$  = displacement.

So we have

$$\{\sigma\} = [D]\{\varepsilon\} \tag{5}$$

where  $\{\sigma\}$  = stress;  $[D]$  = constitutive matrix; and  $\{\varepsilon\}$  = strain.

$$\int_v \{\delta\varepsilon\}[D]\{\varepsilon\} dv = \{\delta d\} \int_v [B]^T [D] [B] dv \{d\} + \{d\} \int_v [\delta B]^T \{\delta\} dv \tag{6}$$

The first term on the right-hand side of Eq. (6) is the usual material stiffness matrix  $[K_0]$ . The second term, which represents the effect of geometrical nonlinearity, is known as the geometric stiffness matrix  $[K_\sigma]$ .

The basic equilibrium equation for large deformations and material nonlinearity takes on nonlinear relationship and its solution cannot be solved directly. An approximate solution can be obtained by referring all variables to a previously calculated known equilibrium configuration and linearizing the resulting equation. This solution can then be improved by iteration.

#### 4. Model for laminated rubber bearings

Laminated rubber bearings have the ability to support a high load in compression and to accommodate one or more movements in shear. The internal construction of the laminated rubber bearings is illustrated in Fig. 6.

A hysteretic model has been recently formulated by the authors for high-damping steel laminated rubber bearings (HDRB). The model has been improved here and used to model the hysteretic behavior of a set of HDRB subject to quasi-static experimental tests. The tests confirmed that the

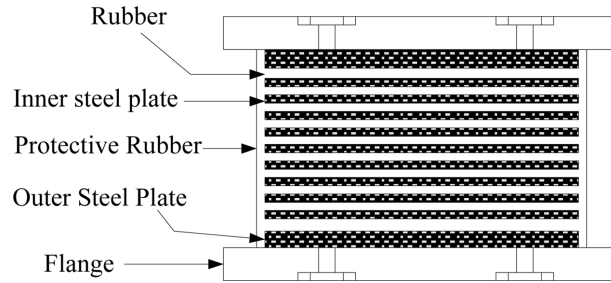


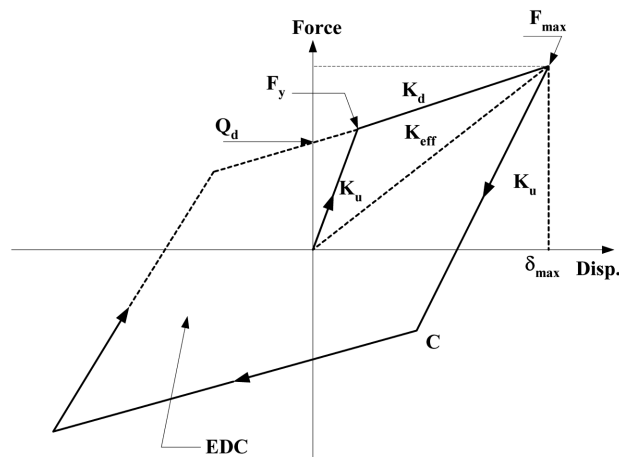
Fig. 6 Laminated rubber bearing

hysteretic behavior strongly depends on geometrical and mechanical characteristics of the isolator (Hwang *et al.* 2002).

#### 4.1 Nonlinear material model for seismic isolator

Mathematical models of laminated rubber bearings under cyclic loading have been proposed on the basis of experimental data (Hwang *et al.* 2002, Abe *et al.* 2004). Of these models, an elastoplastic model is extended by adding the displacement-dependent isotropic hardening rule and the parallel nonlinear elastic spring. Furthermore, the equivalent stiffness and damping ratio of the model are derived in the analytical forms, which are useful for the design. The numerical algorithm has been used to verify, through some numerical examples, the effectiveness of base isolation in reducing the potential structural damage.

An analytical model of the laminated rubber bearings is proposed by extending the elastoplastic model (see Fig. 7). The model is found to accurately simulate the seismic response observed in the experiment.



$Q_d$  : Characteristic Strength,  $F_y$  : Yield Force,  $F_{max}$  : Maximum Force,  
 $K_d$  : Post-yield Stiffness,  $K_{eff}$  : Effective Stiffness,  $K_u$  : Elastic Stiffness,  
 $\delta_{max}$  : Maximum Bearing Displacement, EDC : Area of Hysteresis Loop

Fig. 7 Hysteresis loop of bilinear model

Laminated rubber bearings provide the initial stiffness  $K_u$  and reliable yield level  $F_y$ . The area of force-deflection loop is a measure of the dissipated energy. Restoring hysteresis loop in a bilinear model is illustrated in Fig. 7. Restoring force can be written in the following form

$$f(d_{iso}) = K_{iso} \cdot d_{iso} + Q_d \tag{7}$$

where  $K_{iso}$  = stiffness matrix of isolation bearings;  $d_{iso}$  = displacement of isolation bearings; and  $Q_d$  = characteristic strength.

The bilinear model can be used to perform earthquake analyses following hysteresis loops of isolators in each time step, and the equivalent linearization model can be used to perform earthquake analyses with equivalent stiffness and damping for the total analysis time.

#### 4.2 Formulation for seismic isolator element

The seismic isolator element was developed for the inelastic finite element analyses of reinforced concrete bridge piers supported by laminated rubber bearings. The stress and strain of the seismic isolator can be obtained by using a 3-dimensional spring element when the isolator is modeled as an independent element. The formulation of the element requires coordinate transformation from the element coordinate system to the reference coordinate system.

The element stiffness matrix of isolation bearings is written, as shown in Fig. 8. The element stiffness matrix is derived from the above mentioned material model for laminated rubber bearings (see Fig. 7). The element stiffness matrix is also defined in the global coordinates. The mass of isolation bearings is not considered. But, the stiffness of isolation bearings in the direction of the earthquake changes in each time step.

|       |       |       |       |       |       |        |        |        |        |        |        |
|-------|-------|-------|-------|-------|-------|--------|--------|--------|--------|--------|--------|
| $K_x$ |       |       |       |       |       | $-K_x$ |        |        |        |        |        |
|       | $K_y$ |       |       |       |       |        | $-K_y$ |        |        |        |        |
|       |       | $K_z$ |       |       |       |        |        | $-K_z$ |        |        |        |
|       |       |       | $R_x$ |       |       |        |        |        | $-R_x$ |        |        |
|       |       |       |       | $R_y$ |       |        |        |        |        | $-R_y$ |        |
|       |       |       |       |       | $R_z$ |        |        |        |        |        | $-R_z$ |
|       |       |       |       |       |       | $K_x$  |        |        |        |        |        |
|       |       | Symm. |       |       |       |        | $K_y$  |        |        |        |        |
|       |       |       |       |       |       |        |        | $K_z$  |        |        |        |
|       |       |       |       |       |       |        |        |        | $R_x$  |        |        |
|       |       |       |       |       |       |        |        |        |        | $R_y$  |        |
|       |       |       |       |       |       |        |        |        |        |        | $R_z$  |

$K_x$  : longitudinal direction -  $K_u$  or  $K_d$   
 $K_z$  : transverse direction -  $K_u$  or  $K_d$

Fig. 8 Element stiffness matrix of isolation bearings

## 5. Nonlinear finite element analysis program (RCAHEST)

RCAHEST is a nonlinear finite element analysis program for analyzing reinforced concrete structures. The program was developed by Kim and Shin (2001), at the Department of Civil and Environmental Engineering, Sungkyunkwan University. The program is used to model various reinforced concrete structures under a variety of loading conditions.

The proposed structural element library RCAHEST is built around the finite element analysis program shell named FEAP, developed by Taylor (2000). FEAP is characterized by modular architecture and by the facility that is used to introduce the type of custom elements, input utilities, and custom strategies and procedures.

The elements developed for the nonlinear finite element analyses of reinforced concrete bridge piers are a reinforced concrete plane stress element and an interface element (Kim and Shin 2001, Kim *et al.* 2002, 2003, 2005, 2006).

Accompanying the present study, the authors attempt to implement a seismic isolator element for the laminated rubber bearings.

## 6. Numerical examples

The data for the reinforced concrete bridge piers supported by laminated rubber bearings by Shoji *et al.* (2001) were used to verify the applicability of the proposed method. Cyclic loading tests were conducted to clarify the relation of plastic deformations between a rubber bearing and a reinforced concrete bridge pier. With the experimental results, implementation of the bearing to different type of bridge piers was investigated through numerical simulation.

### 6.1 Description of test specimens

Experimental testing of structures to assess their seismic performance during severe earthquakes requires decisions about the appropriate displacement history to be imposed for seismic loading simulation.

The mechanical properties of the specimens are listed on Table 1 and Table 2, and the geometric

Table 1 Test specimens (Shoji *et al.* 2001)

| Item  | TP-18, TP-19        | TP-20               |
|---|---------------------|---------------------|
| Section size (mm)                           | 400 × 400           | 400 × 400           |
| Column height (mm)                          | 1850                | 1750                |
| Effective depth (mm)                        | 360                 | 360                 |
| Longitudinal reinforcement ratio (%)        | 0.95                | 0.99                |
| Volumetric ratio of tie reinforcement (%)   | 0.77                | 0.77                |
| Cylinder strength of concrete (MPa)         | 20.6                | 29.1                |
| Longitudinal reinforcement (Yield Strength) | SD295A D13 (367MPa) | SD295A D16 (374MPa) |
| Tie reinforcement (Yield Strength)          | SD295A D6 (376MPa)  | SD295A D6 (363MPa)  |
| Axial force (kN)                            | 192 (1.23MPa)       | 192 (1.23MPa)       |

Table 2 Properties of laminated rubber bearing (Shoji *et al.* 2001)

|   |                         |
|---|-------------------------|
| Cross section size (mm)                         | 270 × 270               |
| Effective size (mm)                             | 250 × 250               |
| Thickness of HDR bearing (mm)                   | 61                      |
| Thickness of rubber                             | 13 mm @ 4 Layer = 52 mm |
| Thickness of steel plate                        | 3 mm @ 3Layer = 9 mm    |
| Maximum reaction force (kN)                     | 160                     |
| Minimum reaction force (kN)                     | 100                     |
| Design displacement (mm)                        | 80                      |
| Effective design displacement (mm)              | 56                      |
| Shear modulus (MPa)                             | 1.2                     |
| Yield displacement (mm)                         | 7.0                     |
| Yield force (kN)                                | 30                      |
| Initial stiffness (Elastic Stiffness) (kN/mm)   | 4.29                    |
| Second stiffness (Post-yield Stiffness) (kN/mm) | 0.914                   |

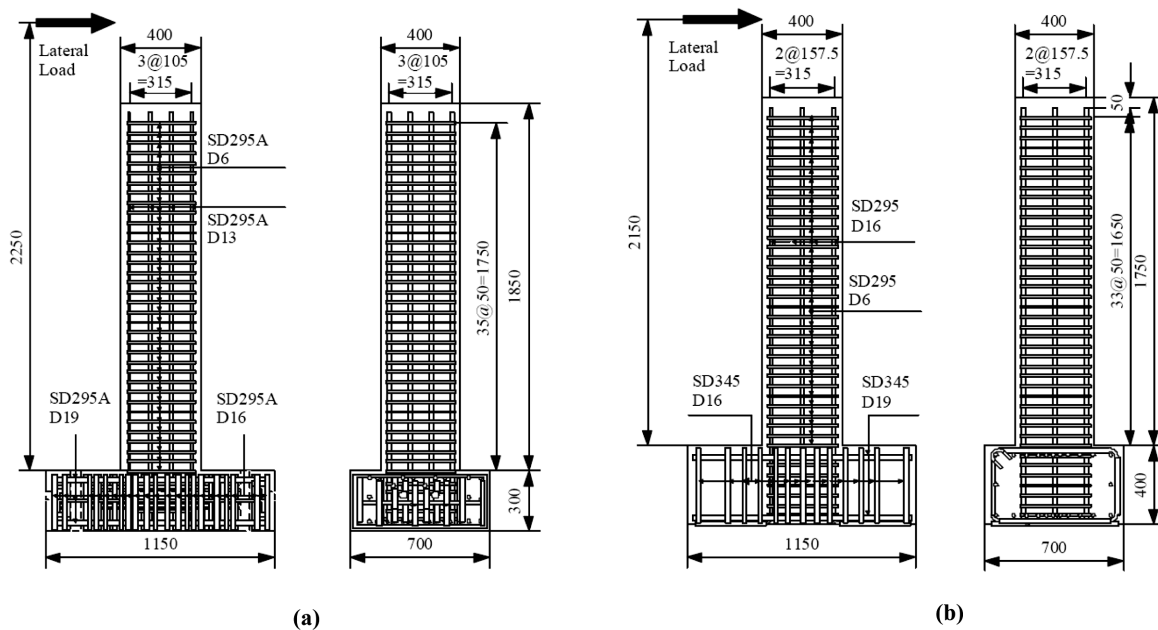


Fig. 9 Test specimens (Unit: mm) (Shoji *et al.* 2001): (a) TP-18, TP-19, (b) TP-20

details are shown in Fig. 9 through Fig. 11. Specimen names in the tables are those used by Shoji *et al.* (2001). All specimens are tested under constant compressive axial load.

A displacement-controlled quasi-static cyclic load tests have been carried out. Fig. 12 shows the cyclic load history, which was based on the lateral displacement pattern of increasing yield displacement. More detailed descriptions of both schemes are available in Reference (Shoji *et al.* 2001).

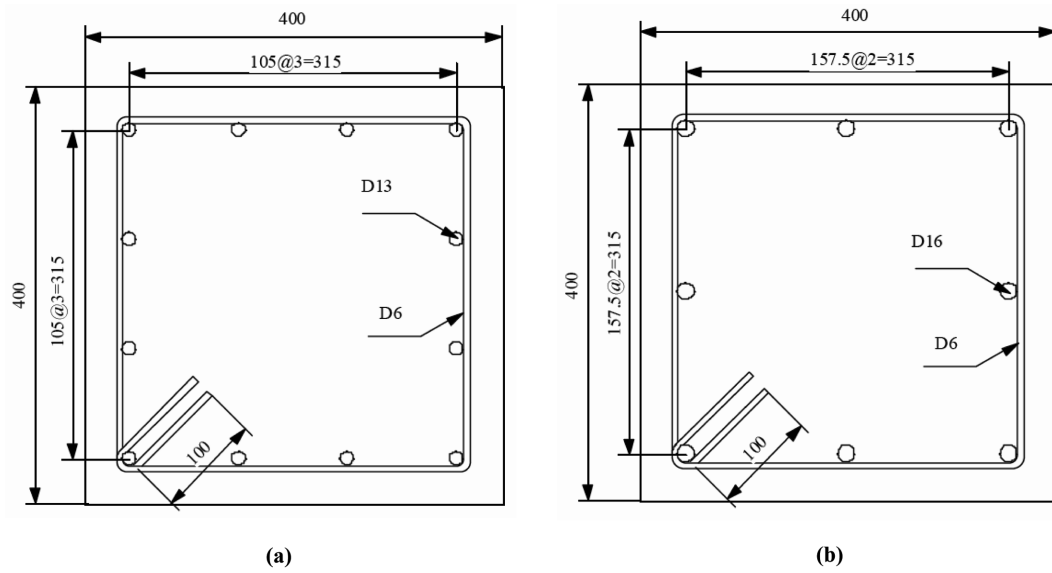


Fig. 10 Cross section (Unit: mm) (Shoji *et al.* 2001): (a) TP-18, TP-19, (b) TP-20

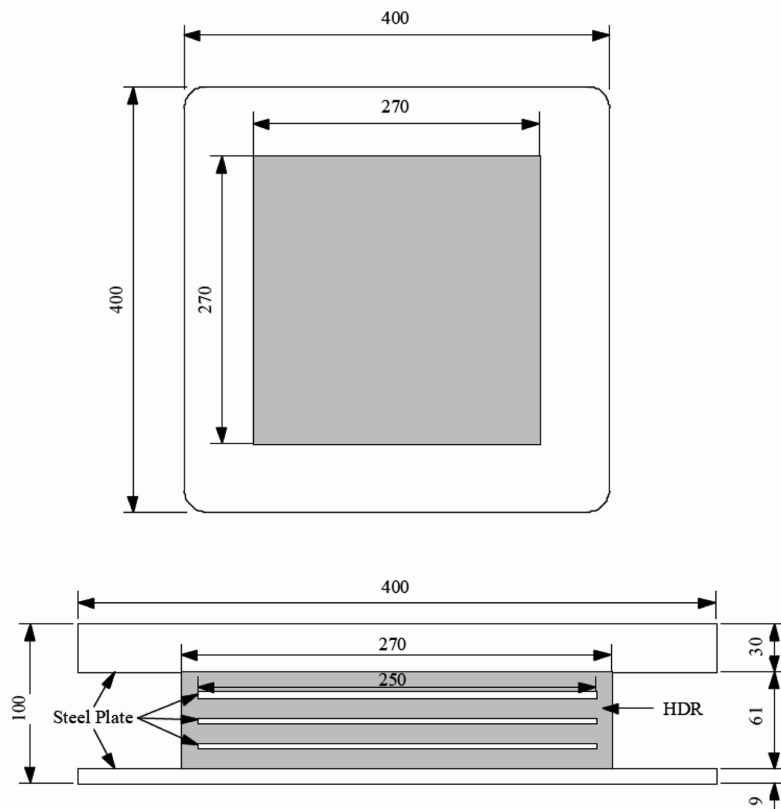


Fig. 11 Laminated rubber bearing (Unit: mm) (Shoji *et al.* 2001)

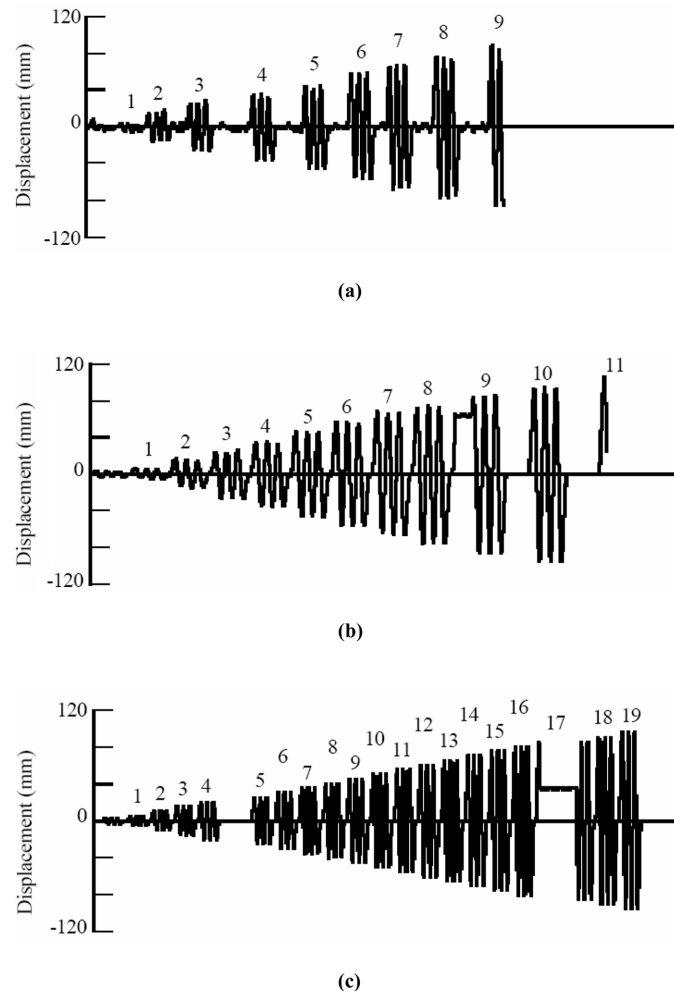


Fig. 12 Loading hysterereses (Shoji *et al.* 2001): (a) TP-18; (b) TP-19, (c) TP-20

## 6.2 Description of analytical model

Fig. 13 shows the finite element discretization and the boundary conditions for seismic analyses of reinforced concrete bridge pier specimens. The interface elements between the footing and the column enhance the modeling of the effects of the bond-slip of steel bars and the local compression. The seismic isolator element is also used to describe the inelastic behaviors of laminated rubber bearings. Numerical loading is applied by incrementing horizontal displacement at the same position as in the experiment. According to the loading condition, the boundary condition such as translation is changed at the loading point.

For a column subjected to axial load, the P-delta effect was expected to play a crucial role on the load-displacement behavior. In the analysis, geometrical nonlinearity was considered to account for the P-delta effect, which may play a crucial role for large deformation. The analysis takes into account both material nonlinearity and geometrical nonlinearity by the total Lagrangian formulation.

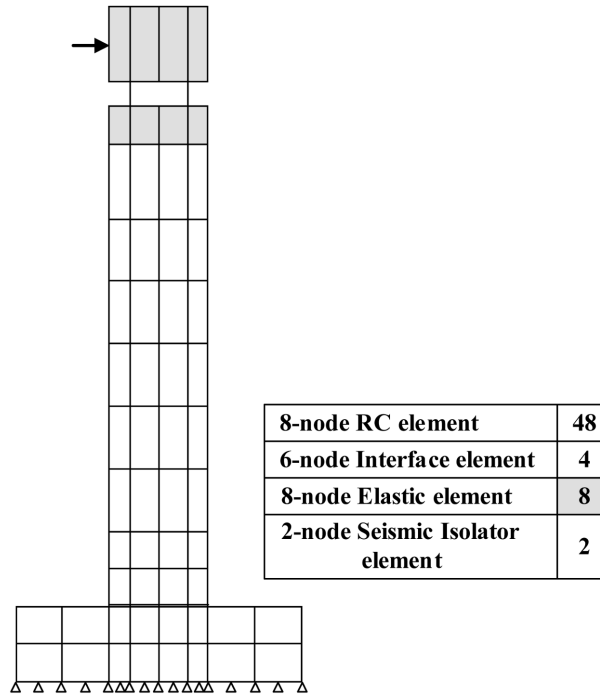


Fig. 13 Finite element mesh for reinforced concrete bridge piers supported by laminated rubber bearings

The reinforcement buckling and cover spalling were considered. The pullout of reinforcing bars from the footing was also considered by placing the interface element at the column-footing interface.

### 6.3 Comparison with experimental results

Fig. 14 shows a comparison between the experimental and analytical behavior for this test. The analytical results show reasonable correspondence with the experimental results. The analysis not only predicted the stiffness, load, and deformation at the peak correctly but also captured the post-peak softening well. However, the analytical cyclic loops exhibit higher residual displacement and energy dissipation than experiment. This may be due to using the bilinear hysteresis model for the laminated rubber bearings.

Fig. 15 shows load-displacement envelopes for experimental and analytical results of specimens. For each of the test bridge piers, the predicted and the measured maximum loads were in good agreement. The proposed model provides a realistic prediction of deflections at given loads for all piers.

Seismic performance of reinforced concrete bridge piers can be evaluated as displacement ductility. The ductility of reinforced concrete bridge piers is associated with shear and flexural carrying capacities. The ductility of reinforced concrete bridge piers supported by laminated rubber bearings may also be simulated by using finite elements.

The load-displacement hysteresis for the bearing and the load-displacement hysteresis for the reinforced concrete column can be separated from the load-displacement hysteresis for specimen

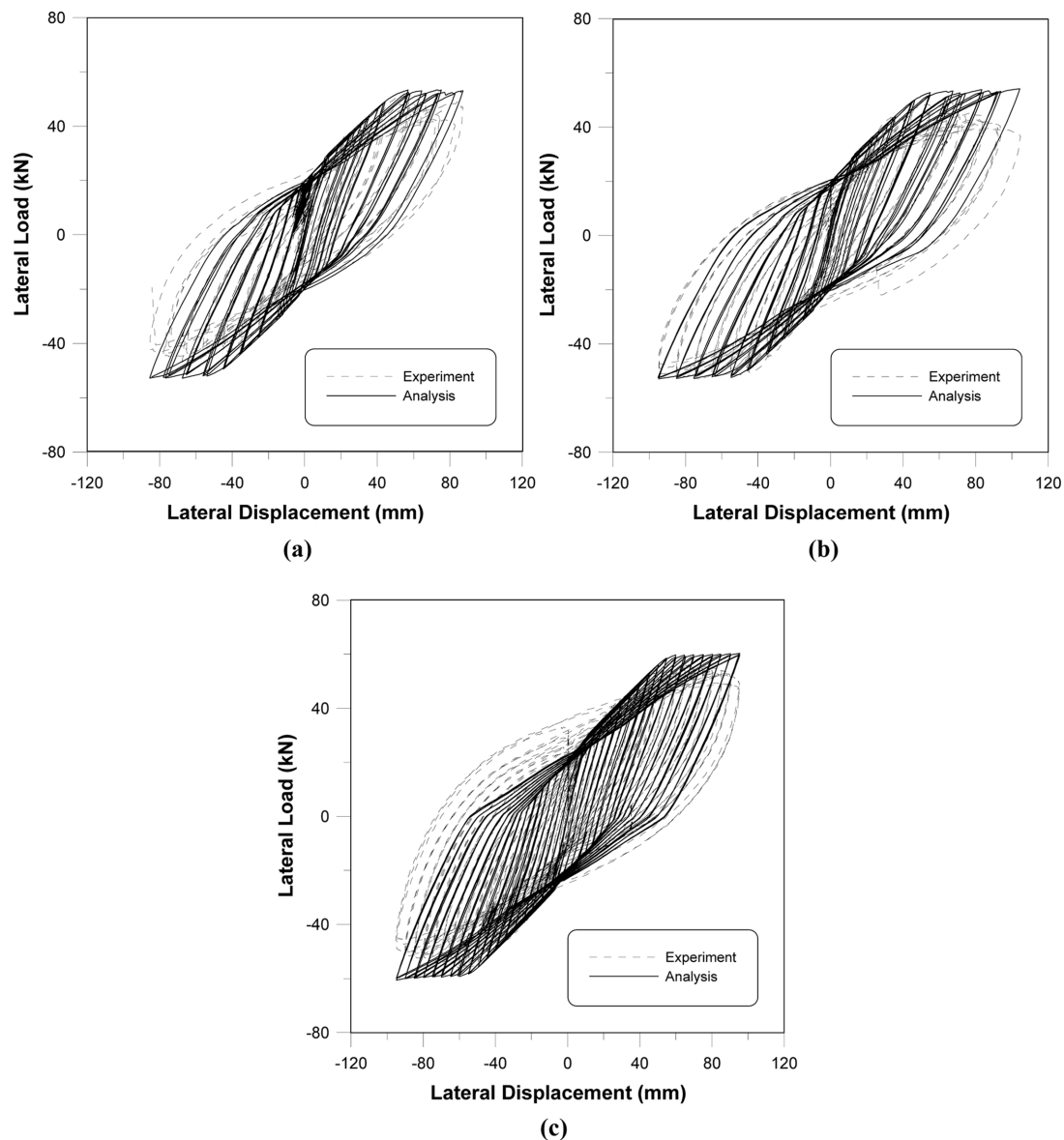


Fig. 14 Load-displacement curve: (a) TP-18, (b) TP-19, (c) TP-20

TP-19 (see Fig. 14(b)). Figs. 16 through 19 compare the hystereses for selected lateral displacements. Figures depict the comparison for specimen TP-19 with hysteresis and displacement varying from 15 mm to 95 mm, respectively. Figures show how the displacements developed in the reinforced concrete column, and the laminated rubber bearing are correlated in a loading cycle. The lateral displacement at the loading point consists of the lateral displacements of the reinforced concrete column and the laminated rubber bearing.

As observed in Figs. 16-19, good agreement is obtained between the experimental and numerical results. Because the yield strength of the laminated rubber bearing is much lower than the yield

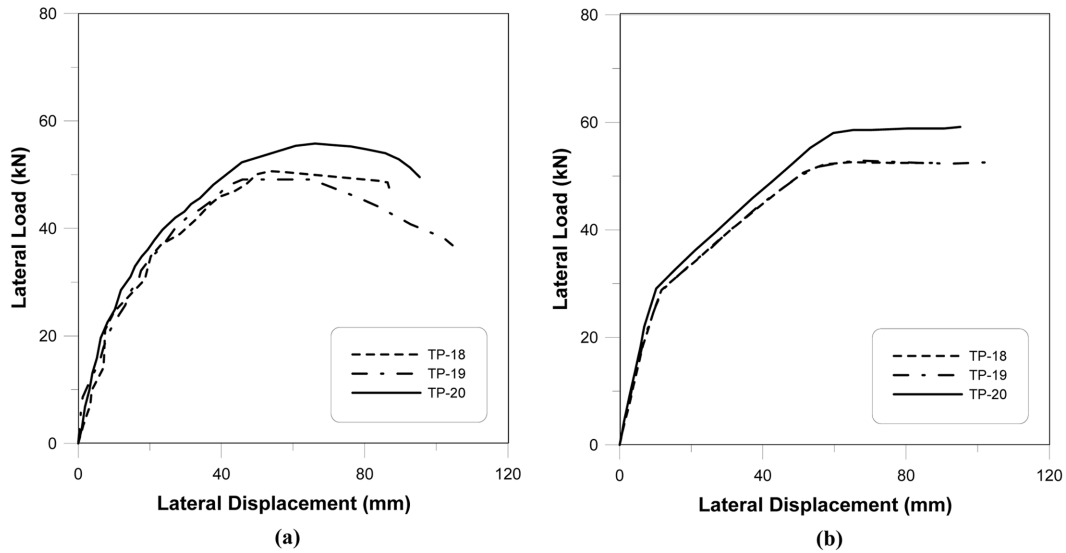


Fig. 15 Load-displacement envelopes for specimens: (a) Experiment, (b) Analysis

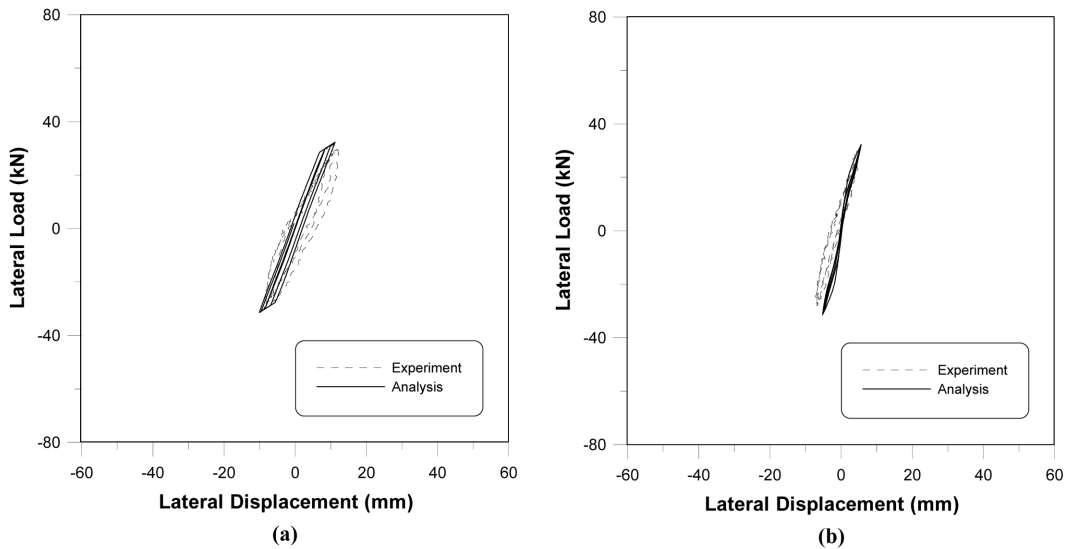


Fig. 16 Load-displacement hysteresis for specimen TP-19 (15 mm): (a) Laminated rubber bearing, (b) foundation-pier

strength of the reinforced concrete column, the plastic deformation of the pier system occurs mainly due to the plastic deformation of the laminated rubber bearing under lower loading cycles as shown in Fig. 16 and Fig. 17. After yielding of the reinforced concrete column, the plastic deformation of the pier system consists of the plastic deformation of the reinforced concrete column and the laminated rubber bearing. From the experimental and analytical results in Fig. 18 and Fig. 19, it is found that the large plastic deformation occurs in the pier system due to the plastic deformation of the reinforced concrete column as well as the laminated rubber bearing. It is important to note that

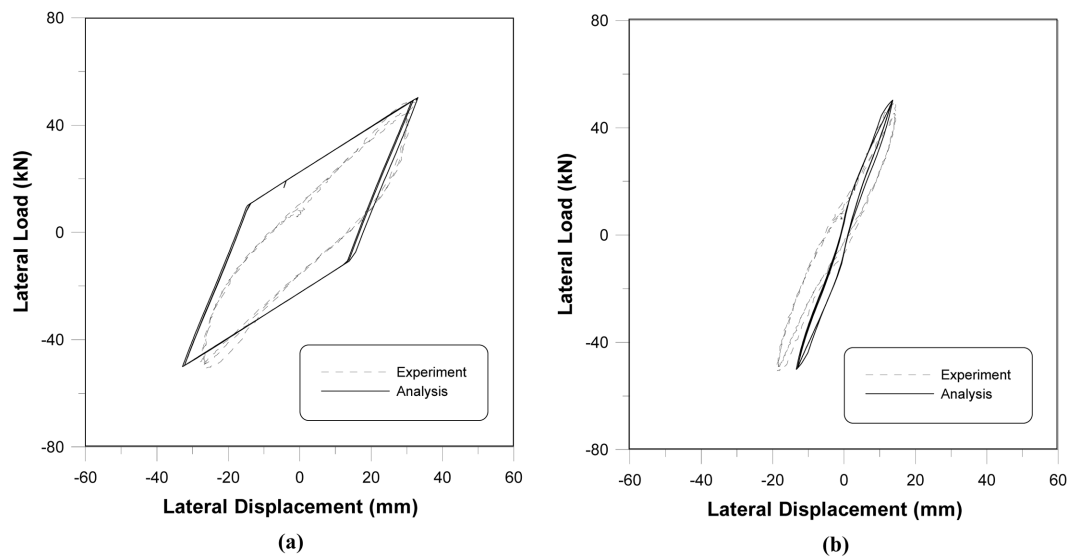


Fig. 17 Load-displacement hysteresis for specimen TP-19 (45 mm): (a) Laminated rubber bearing, (b) foundation-pier

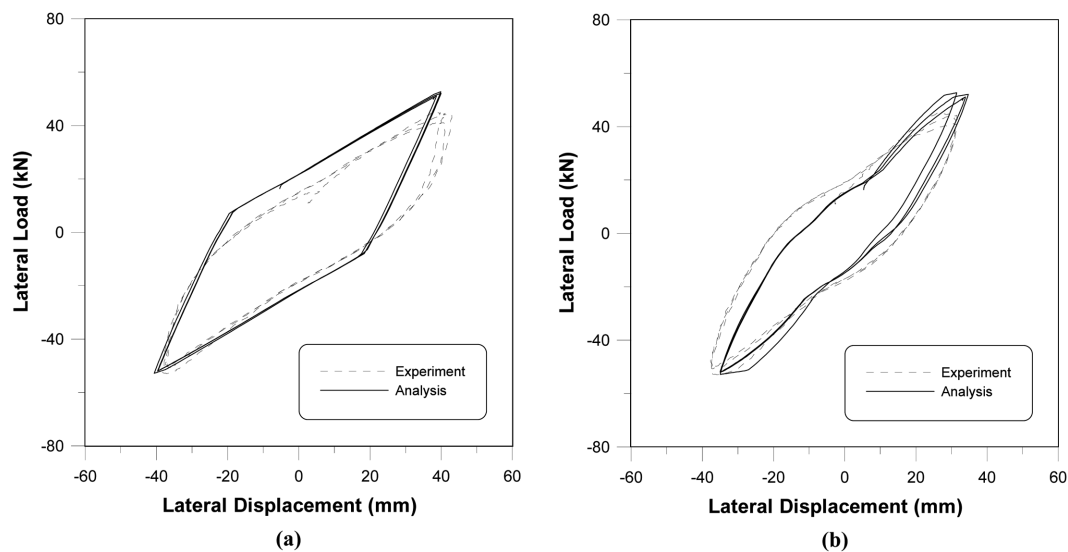


Fig. 18 Load-displacement hysteresis for specimen TP-19 (75 mm): (a) Laminated rubber bearing, (b) foundation-pier

such a large plastic deformation occurs in the pier in an isolated system. However, there are some discrepancies in the results which, in addition to the modeling idealizations, may be caused by several sources of inaccuracy, such as those related to the variability of assumed material characteristics. Nevertheless, the comparisons clearly demonstrate the overall accuracy and reliability of the analytical model in predicting the structural response of reinforced concrete bridge piers supported by laminated rubber bearings.

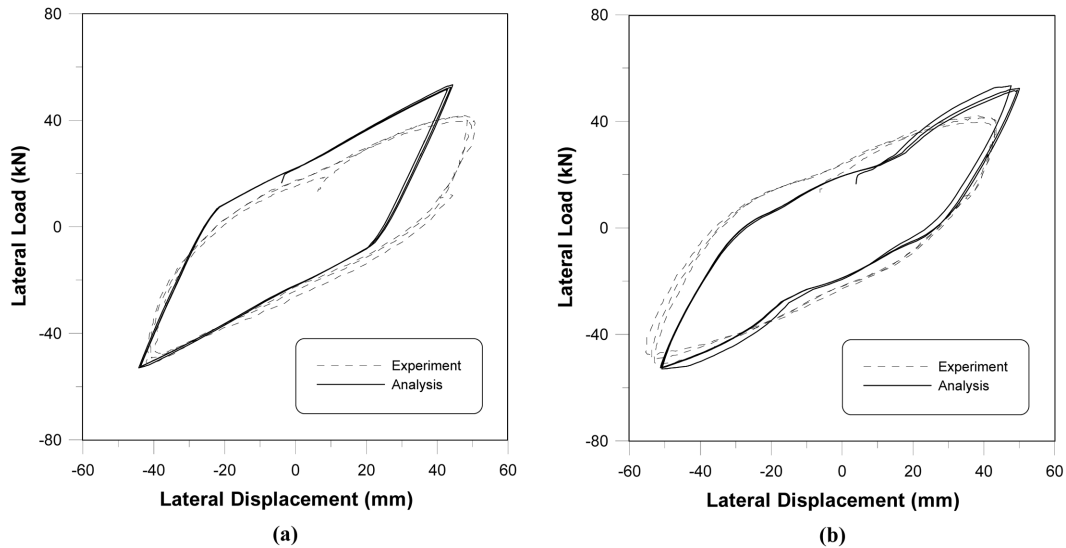


Fig. 19 Load-displacement hysteresis for specimen TP-19 (95 mm): (a) Laminated rubber bearing, (b) foundation-pier

## 7. Conclusions

This paper presents a new method for the nonlinear analysis of reinforced concrete bridge piers supported by laminated rubber bearings, accounting for geometric and material nonlinearities. Theory and formulations for analytical models to be implemented with numerical methods for predicting the behavior of reinforced concrete bridge piers supported by laminated rubber bearings are described. The agreement between the numerical simulations and experimental findings demonstrate the overall accuracy and reliability of the analytical models in predicting the response of reinforced concrete bridge piers supported by laminated rubber bearings. It is expected that, by using the proposed models, the seismic response of reinforced concrete bridge piers can be predicted accurately, and this enables more rational and reliable design of bridge piers. From the results of the numerical simulations and comparisons with experimental data, the following conclusions are reached.

1. The proposed constitutive model and numerical analysis describe the inelastic behavior of the reinforced concrete bridge piers supported by laminated rubber bearings with acceptable accuracy and the method may be used in the seismic design of reinforced concrete bridge piers.
2. The developed seismic isolator element seems to give a good prediction of inelastic behavior of laminated rubber bearings.
3. A model of laminated rubber bearings is proposed. The model consists of an elastoplastic spring to express the characteristics such as the strain dependency, maximum strain dependency, and hardening property. The model is found to well approximate the restoring forces of laminated rubber bearings.
4. Nonlinear finite element analysis may be used to investigate the design details and the load-deflection responses of reinforced concrete bridge piers supported by laminated rubber bearings. Also, failure modes and ductility may be checked for seismic resistant design.

5. Certain procedures should be included in the current design codes to guide the engineers toward an acceptable method for evaluating the available strength in existing reinforced concrete bridge piers supported by laminated rubber bearings.

## Acknowledgements

The study described in this paper was supported by the Ministry of Land, Transport and Maritime Affairs through the Korea Bridge Design and Engineering Research Center. The authors wish to express their gratitude for the support received. We are especially grateful to Prof. Kazuhiko Kawashima for offering test results.

## References

- Abe, M., Yoshida, J. and Fujino, Y. (2004), "Multiaxial behaviors of laminated rubber bearings and their modeling. II: Modeling", *J. Struct. Eng.*, ASCE, **130**(8), 1133-1144.
- American Association of State Highway and Transportation Officials (1999), *AASHTO Guide Specifications for Seismic Isolation Design*.
- Bathe, K.J. (1996), *Finite Element Procedures*, Prentice-Hall, Inc.
- Chen, B.J., Tsai, C.S., Chung, L.L. and Chiang, T.C. (2006), "Seismic behavior of structures isolated with a hybrid system of rubber bearings", *Struct. Eng. Mech.*, **22**(6), 761-783.
- Hwang, J.S., Wu, J.D., Pan, T.C. and Yang, G. (2002), "A mathematical hysteretic model for elastomeric isolation bearings", *Earthq. Eng. Struct. Dyn.*, **31**, 771-789.
- Juhn, G., Manolis, G.D., Constantinou, M.C. and Reinhorn, A.M. (1992), "Experimental study of secondary systems in base-isolated structure", *J. Struct. Eng.*, ASCE, **118**(8), 2204-2221.
- Kakuta, Y., Okamura, H. and Kohno, M. (1982), "New concepts for concrete fatigue design procedures in Japan", *IABSE Colloquium of Fatigue of Steel and Concrete Structures*, Lausanne, 51-58.
- Kato, B. (1979), "Mechanical properties of steel under load cycles idealizing seismic action", *CEB Bulletin D'Information*, **131**, 7-27.
- Kim, T.H., Kim, B.S., Chung, Y.S. and Shin, H.M. (2006), "Seismic performance assessment of reinforced concrete bridge piers with lap splices", *Eng. Struct.*, **28**(6), 935-945.
- Kim, T.H., Lee, K.M., Chung, Y.S. and Shin, H.M. (2005), "Seismic damage assessment of reinforced concrete bridge columns", *Eng. Struct.*, **27**(4), 576-592.
- Kim, T.H., Lee, K.M. and Shin, H.M. (2002), "Nonlinear analysis of reinforced concrete shells using layered elements with drilling degree of freedom", *ACI Struct. J.*, **99**(4), 418-426.
- Kim, T.H., Lee, K.M., Yoon, C.Y. and Shin, H.M. (2003), "Inelastic behavior and ductility capacity of reinforced concrete bridge piers under earthquake. I: Theory and formulation", *J. Struct. Eng.*, ASCE, **129**(9), 1199-1207.
- Kim, T.H. and Shin, H.M. (2001), "Analytical approach to evaluate the inelastic behaviors of reinforced concrete structures under seismic loads", *J. Earthq. Eng. Soc. Korea*, EESK, **5**(2), 113-124.
- Li, B., Maekawa, K. and Okamura, H. (1989), "Contact density model for stress transfer across cracks in concrete", *J. Faculty Eng.*, University of Tokyo (B), **40**(1), 9-52.
- Maekawa, K. and Okamura, H. (1983), "The deformational behavior and constitutive equation of concrete using elasto-plastic and fracture model", *J. Faculty Eng.*, University of Tokyo (B), **37**(2), 253-328.
- Mander, J.B., Panthaki, F.D. and Kasalanati, K. (1994), "Low-cycle fatigue behavior of reinforcing steel", *J. Mater. Civil Eng.*, ASCE, **6**(4), 453-468.
- Mander, J.B., Priestley, M.J.N. and Park, R. (1988), "Theoretical stress-strain model for confined concrete", *J. Struct. Eng.*, ASCE, **114**(8), 1804-1826.
- Naeim, F. and Kelly, J.M. (1999), *Design of Seismic Isolated Structure from Theory to Practice*, John Wiley & Sons, Inc.

- Okamura, H., Maekawa, K. and Izumo, J. (1987), "RC plate element subjected to cyclic loading", *IABSE Colloquium*, Delft, **54**, 575-590.
- Roeder, C.W. and Stanton, J.F. (1991), "State-of-the-art elastomeric bridge bearing design", *ACI Struct. J.*, **88**(1), 31-41.
- Shima, H., Chou, L. and Okamura, H. (1987), "Micro and macro models for bond behavior in reinforced concrete", *J. Faculty Eng.*, University of Tokyo (B), **39**(2), 133-194.
- Shoji, G., Kawashima, K. and Saito, A. (2001), "Cyclic loading test to clarify nonlinear behavior of an isolated bridge supported by high damping rubber bearings", *J. Struct. Mech. Earthq. Eng.*, JSCE, **682**(I-56), 81-100 (in Japanese).
- Skinner, R.I., Robinson, W.H. and McVerry, G.H. (1993), *An Introduction to Seismic Isolation*, John Wiley & Sons.
- Taylor, R.L. (2000), *FEAP – A Finite Element Analysis Program*, version 7.2 users manual, Vols 1-2.
- Yalcin, C. and Saatcioglu, M. (2000), "Inelastic analysis of reinforced concrete columns", *Comput. Struct.*, **77**(5), 539-555.